Stark-width measurements of neutral and singly ionized magnesium resonance lines in a wall-stabilized arc

Claudine Goldbach, Gérard Nollez, Pierre Plomdeur, and Jean-Paul Zimmermann
CNRS, Institut d'Astrophysique, 98 bis Boulevard Arago, 75014 Paris, France
(Received 4 February 1981)

Stark widths of the Mg I 2852.13-Å and of the Mg II 2795.53- and 2802.70-Å resonance lines have been measured in the ranges of electronic density and temperature $1.10-1.64\times10^{17}\,\mathrm{cm}^{-3}$, 12 900–14 300 K. The light source is a stationary, optically thin, wall-stabilized arc burning in argon with a small addition of Mg vapor. Plasma parameters are measured with the use of line and continuum radiation of the argon plasma. Optical depth measurements are performed at the peaks of the investigated lines, and the Mg concentration is continuously controlled to minimize the reabsorption. High spectral resolution is achieved by use of a piezoelectric scanned Fabry-Pérot interferometer whose instrumental profile is measured and found to be Voigt shaped. The experimental profiles are analyzed using a least-squares fit of the Voigt function to all profile intensity points. The Stark width of the Mg I resonance line is found to be 30 to 50% lower than the existing semiclassical calculations. No quantum calculations and no other experimental values are available. As to the Mg II resonance doublet, its width is found lower by a factor of 2 than all the previous experimental values but those of Roberts and Barnard, and our value agrees well with the full quantum calculations of Barnes.

I. INTRODUCTION

The resonance line profiles of neutral and singly ionized magnesium are of particular interest in astrophysics and are investigated in a number of spatial experiments (see, for example, Refs. 1,2). In contrast no laboratory measured Stark profile of the Mg I resonance line at 2852.13 Å is published although the disagreement between various semiclassical calculations[3–5] ranges from 30 to 50% depending on the temperature. As to the Mg II resonance doublet at 2795.53 and 2802.70 Å, its Stark width is calculated through a semiclassical approach[6–9] as well as through a full quantum-mechanical approach.[10,11] The widths measured by Chapelle and Sahal-Bréchot,[7] Jones *et al.*,[12] Hadžiomerspahić *et al.*,[13] and Fleurier *et al.*[9] agree well with the semiclassical calculations of Jones, Benett, and Griem[6] and Sahal-Bréchot[7,9] over a large range of temperature. But the quantum results of Barnes,[11] which lie a factor of 2 lower, are very well fitted by the experimental results of Roberts and Barnard.[8]

This rather confused situation which calls for new accurate experimental data is probably the consequence of two main difficulties encountered in the measurement of these line profiles. First, resonance lines are very sensitive to the reabsorption which distorts their shape and must be carefully minimized. Second, the Stark width being very small (typically a few hundredths of an angström at $n_e=10^{17}\ \mathrm{cm}^{-3}$), the spectral resolution and the profile analysis in terms of the various broadening mechanisms become crucial points.

We present hereafter width measurements of the Mg I and Mg II resonance lines emitted from a stationary, optically thin, wall-stabilized arc plasma. The magnesium is confined to the mid zone of the argon plasma and its concentration is continuously controlled and minimized. The optical depth at the line peaks is directly measured by a double-path method. High spectral resolution is achieved by use of a Fabry-Pérot interferometer whose instrumental broadening is measured and taken into account in the deconvolution procedure.

II. EXPERIMENTAL DEVICE

A. The arc source

Mg I and Mg II resonance radiation is excited in a wall-stabilized arc burning in argon at normal pressure between four thoriated anodes and cathodes (12 insulated water-cooled copper plates

5.5-mm thick, plasma length 75 mm, plasma diameter 5 mm, current between 50 and 200 A). The plasma column may be spectroscopically investigated side-on all along the axis as well as end-on. The gas may get in (out) the arc column at every interplate space.

Pure magnesium is heated in a well-regulated furnace up to a temperature of about 450 °C, corresponding to a magnesium partial pressure around 10-μm Hg.[14] Pure argon flows through the furnace and carries out the magnesium vapor to the arc through a heated copper pipe. The argon-magnesium mixture enters the arc at the middle of the column (typical flow rate 60 l/h), whereas a reverse flow of pure argon enters the arc between the two last plates at both ends and through the electrodes. As it appears from side-on observations, the magnesium atoms do not diffuse far from their admission point and the electrode zones remain free of magnesium.

After a thermal-stabilization period of the furnace at the selected temperature, the stability of the magnesium radiation, measured at the peak intensity of the resonance lines, is better than 5% over several hours. The magnesium concentration in the plasma (deduced from absolute intensity measurements of Mg II resonance lines) is very sensitive to the furnace temperature which is the main parameter to be controlled when looking for optically thin lines. A relative concentration of Mg II to neutral argon atoms of the order of 10^{-6} ensures a sufficient signal level together with a negligible reabsorption in the resonance lines without any disturbance of the arc stability.

B. Optical setup: Data acquisition

As can be seen on Fig. 1, the arc plasma can be observed either end-on or side-on by a 90° rotation around a vertical axis. The plasma column can be investigated through the five side windows owing to a horizontal translation of the arc. Radial scans for Abel inversion are achieved by a vertical displacement of the arc by means of a stepping motor (0.01-mm steps).

On the anode side a small 0.2-m monochromator with a 1200 lines/mm holographic concave grating serves for registering continuously the intensity at the peak of the investigated line and then for checking the stability. For direct absorption measurements, the plane mirror M_1 can be replaced by a concave mirror M_2 whose center of curvature is the midpoint of the plasma.

On the cathode side, the midpoint of the plasma is focused using a spherical mirror (magnification 1:1, beam aperture 1:120) on the entrance slit of a 2-m monochromator with a 600 lines/mm grating working in the first order. The field stop is defined by the circular entrance slit, 0.2 mm in diameter. This monochromator with a variable exit-slit width serves to isolate a given spectral line for further analysis by the Fabry-Pérot interferometer. Higher orders of the grating are eliminated using a high-pass filter.

The parameters describing the plane Fabry-Pérot interferometer (FPI) are listed in Table I. The plate separation is adjustable and for this work is put equal to 0.6 mm in order to minimize the overlapping of adjacent interference orders (free spectral range $\simeq$ six times the width of the line). The plate separation is measured with a traveling microscope. The spectral scanning is obtained by continuously varying the plate separation by means of piezoelectric cylinders. The final parallelism is achieved through fine piezoelectric adjustments. For the registration of the profile, a 200-s rise time of the ramp generator is chosen. Typically seven interference orders are scanned and the profiles retained for data analysis correspond to a scan linearity better than 1% (measured from two successive free spectral ranges). Short rise times (50

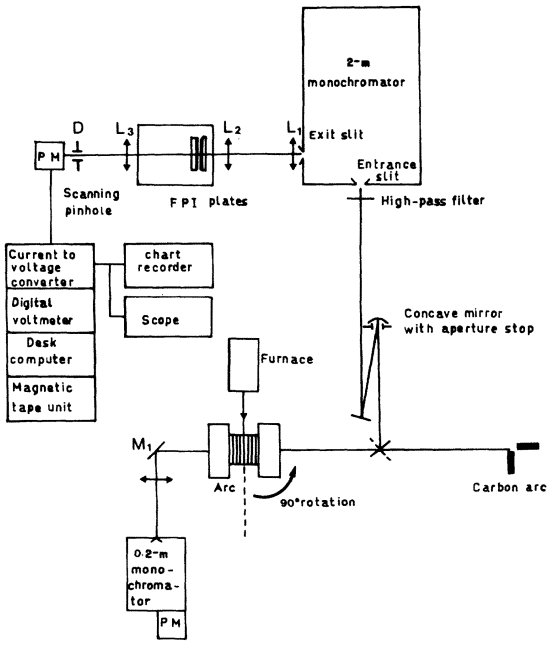

FIG. 1. Schematic diagram of the experimental setup.

TABLE I. FPI parameters ($\lambda=2800$ Å).

Plate diameter	25.4 mm
Working aperture	<10 mm
Flatness	$\lambda/100$ at full aperture Better than $\lambda/200$ at the working aperture
Plate reflectivity	$>97\%$
Reflectivity finesse	>100
Plate separation	Continuously adjustable between 0 and 125 mm
Working plate separation	0.6 mm
Free spectral range	0.6533 Å
Spectral scan	Piezoelectric
Scan parallelism	Better than $\lambda/200$

ms), with the visualization of the interference pattern on a scope, make the parallelism adjustment and control very easy.

As described by Chabbal,[15] the afocal system (L_1,L_2) (magnification 2:1) together with the collimator L_3, conjugates the grating with the pinhole D and the exit slit with the FPI plates. The scanning pinhole D (diameter 0.8 mm) isolates a portion of the central fringe. The photomultiplier (S 20 photocathode) is cooled down to -20°C by Peltier effect. A high-linearity photocurrent-to-voltage converter is connected to a digital voltmeter with variable count rate and integration time, whereas a desk computer and a magnetic tape unit allow the data storage. One interference order provides N intensity data (typically $N=60$), each corresponding to a reduced wavelength

$$x_n=(n-1)/(N-1)=\Delta\lambda/\Delta\lambda_{\mathrm{FSR}}\ ,$$

where $\Delta\lambda_{\mathrm{FSR}}$ is the free spectral range. The value of the plate separation e and the relation $\Delta\lambda_{\mathrm{FSR}}=\lambda^2/2e$ yield the absolute wavelength scale.

The optical alignment of the whole system is accomplished by a laser beam sent through the scanning pinhole, while 0.4-mm diameter pinholes inserted in both ends of the arc channel allow a precise definition of the arc axis.

C. Instrumental profile determination

To determine the instrumental profile, as well as to adjust and control the plate parallelism, a low-pressure Mg hollow-cathode lamp is imaged on the entrance slit of the monochromator by means of auxiliary optics. The full instrumental width $\Delta\lambda_I$ of the FPI is given by

$$\Delta\lambda_I=\Delta\lambda_{\mathrm{FSR}}/F_{\mathrm{app}}=\lambda^2/2eF_{\mathrm{app}}\ ,$$

F_{app} being the apparatus finesse. To measure F_{app} the plate separation e is decreased until $\Delta\lambda_I$ becomes larger than the width of the very narrow Mg I or Mg II resonance lines delivered by the hollow-cathode lamp. The line profile measured under these conditions is the instrumental profile and its width $1/F_{\mathrm{app}}$ in a reduced-wavelength scale $\Delta\lambda/\Delta\lambda_{\mathrm{FSR}}$ is independent of the actual working plate separation.

The instrumental profile of a FPI is approximately Voigt-shaped,[16] the reflectivity losses contributing to the Lorentzian width and the other instrumental effects to the Gaussian width. All measured intensity points of the instrumental profile are then fitted by least squares with an approximate Voigt function given by Whiting.[17] The Voigt and Lorentz full widths, the position and intensity of the line peak, are the four free-fitting parameters. Very good fits (i.e., fits with standard deviations on the Voigt and Lorentz widths within 2%) are obtained, confirming that departures of the instrumental profile from Voigt shape are of minor importance. A typical instrumental profile at $\lambda=2802$ Å is shown in Fig. 2 in a reduced-wavelength scale.

The Table II reports the mean results of ten apparatus profile determinations at $\lambda=2802$ and 2852 Å. The quoted reflectivity finesse F_R is the

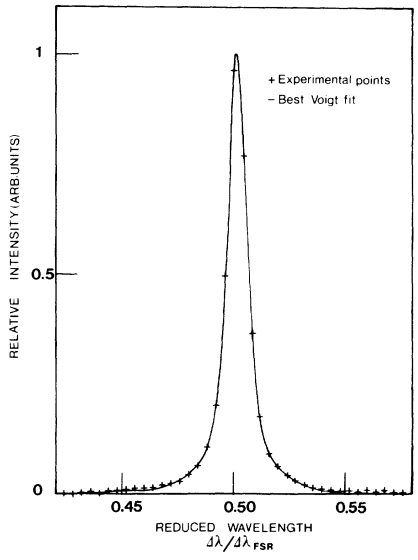

FIG. 2. Typical instrumental profile at $\lambda=2802.70$ Å. The standard deviations on the Voigt and Lorentz widths given by the fitting code are 0.97% and 2.14%, respectively.

TABLE II. Instrumental profile determination. The absolute widths are given for $e=0.6$ mm. The indicated uncertainties are random.

	Apparatus finesse	Reflectivity finesse	Full width of the Voigt profile (Å)	Full Lorentzian width (Å)	Full Gaussian width (Å)
$\lambda=2852.13$ Å	78	88	0.008 68±0.5%	0.007 66±1%	0.0030±4.5%
$\lambda=2802.70$ Å	100	119	0.006 53±0.5%	0.005 50±1.5%	0.0026±4.5%

inverse of the Lorentzian width in the reduced-wavelength scale. The F_{app} values are only 15% lower than the F_R values, showing that the instrumental broadening is effectively minimized. The quoted errors are random and come from the noise in the data (see below the error analysis discussion). As to the systematic error on the Lorentzian width it amounts to $+1\%,-7\%$: the nonlinearity of the scan induces a $\pm1\%$ error, the determination of the experimental width with a non strictly monochromatic line yields a 6% overestimation.

III. PLASMA PARAMETER DETERMINATION

A. Temperature determination

The plasma temperature is deduced from the measured absolute emission coefficients of the Ar I 4300-Å and Ar II 4806-Å lines. To perform these measurements, the photomultiplier is fixed behind the exit slit of the grating monochromator and the intensities are put on an absolute scale by comparison with the radiation of a low-current carbon arc using the data of Magdeburg and Schley.[18] Standard corrections for wing contribution[19] and self-absorption[20] are applied to end-on measurements. Good reproducibility of the emission coefficient values is achieved for given arc current and pressure (typical standard error of the mean of 3% for ten independent determinations).

The values of the transition probabilities are those deduced by Nubbemeyer[21] from emission measurements in a wall-stabilized arc under LTE assumption (Ar I 3.91×10^5 s^{-1}, Ar II 1.02×10^8 s^{-1}). This couple of values ensures a 1% agreement between the temperatures deduced from the two lines. However, to account for the discrepancies (especially for the Ar II line) between Nubbemeyer's results and (i) results obtained under similar experimental conditions,[22,23] and (ii) results deduced from lifetime measurements,[24,25] the uncertainty $\Delta A/A$ is largely overestimated in regard to Nubbemeyer's evaluation (Ar I $\Delta A/A=\pm15\%$, Ar II $\Delta A/A=\pm30\%$).

The temperature measurements are performed either end-on on the plasma axis or side-on at different positions along the plasma column. The side-on measured intensities (40 data over the plasma diameter) are reduced to radial emission coefficients through Abel inversion. The computer code used to perform this inversion is due to Fleurier and Chapelle[26] and involves a smoothing procedure of the measured data using Gram's orthogonal polynomials. The integral is then calculated analytically in a small interval on the right of the discontinuity point; the remaining part is estimated numerically.

Errors in the Abel inverted emission coefficient can reach 20% at $r=0$, which, together with a $\pm5\%$ error in the absolute calibration and the quoted uncertainties in the transition probability values, yield a $\pm3\%$ systematic error in the temperature determination for both lines. The random uncertainty is given by the standard error of the mean value ($\leq0.3\%$) over ten independent determinations.

A small but systematic difference, $T_{end}-T_{side}$, is found between the axis temperatures deduced from end-on and from side-on measurements of the Ar II line, its relative value depending on the abscissa along the plasma axis: at the center it amounts to about -0.3%; at ±20 mm from the center it reaches $+1\%$. These small temperature variations along the axis are due to differences in the constriction of the plasma column. At the center, the in-flow of the Ar + Mg mixture ensures an efficient plasma constriction to 4.8-mm diameter, while at the interplates where no gas is introduced, the plasma bulges and its diameter reaches 6 mm (the plasma edges are defined by a signal level of 10^{-3} of the peak signal). These axial temperature inhomogeneities in a wall-stabilized arc have been studied by Nubbemeyer[27] as a function of the ratio r of the constricted length to the total plasma length. For the value $r=0.9$ corresponding to the arc used in this experiment, he predicts approxi-

TABLE III. Plasma diagnostics, end-on measurements, pressure 1020 mbar. (Because of the too-strong-wings contribution the Ar I 4300-Å line is not used at 140 A.)

	80 A		100 A		140 A	
	T(K)	$n_e(10^{17}$ cm$^{-3})$	T(K)	$n_e(10^{17}$ cm$^{-3})$	T(K)	$n_e(10^{17}$ cm$^{-3})$
Ar I 4300-Å line	12910±390	1.07±0.21	13300±400	1.25±0.25		
Ar II 4806-Å line	13030±390	1.12±0.22	13440±400	1.31±0.26	14260±430	1.64±0.33
Continuum 4000 Å		1.02±0.20		1.25±0.25		1.65±0.33
Mean values	12970±390	1.10±0.22	13370±400	1.28±0.26	14260±430	1.64±0.33

mately a 6.5% underestimation of the Ar II emission coefficient deduced from end-on observations (0.4% underestimation of the temperature) and a negligible influence of the temperature inhomogeneities on the Ar I line emission. These evaluations agree well with our own results.

Furthermore, side-on observations of the Mg II resonance lines along the plasma axis show that magnesium is confined in a small axial region around the plasma center. The influence of the axial temperature inhomogeneities is then very weak having regard to the systematic uncertainty on the temperature and may be ignored.

The temperature values measured on the arc axis, for various currents, at a pressure of 1020 mbar are given in Table III.

B. Electron-density determination

Following standard criteria[28,29] as well as experimental checks,[21,30,31] local thermodynamic equilibrium prevails in such an atmospheric high-current argon arc. The electron density is therefore calculated from the measured temperature through the equilibrium relations. In the temperature range investigated, the ±3% systematic error on T yields a ±18% systematic error on the electron density. The axial inhomogeneities of the electron density in the region of Mg radiation ($\Delta T/T=1.3\%$ corresponding to $\Delta n_e/n_e=8\%$ over 10% of the length) lead to an averaged n_e value along the axis which departs, at most by 1%, from the n_e value deduced from side-on measurements of the temperature at the plasma center. The total systematic error in electron density amounts then to about ±20% (random error ±2%).

The equilibrium results are checked by measuring axially and radially the absolute continuum emission coefficient at $\lambda=4000$ Å, where the ξ value calculated by Hofsaess[32] agrees particularly well with available experimental results[33–35] ($\xi=1.5$). As can be seen in Table III this yields n_e values which depart by 10% at most from the equilibrium values. Moreover the continuous (recombination continuum proportional to n_e^2) is used to test the influence of magnesium addition to the argon plasma by side-on measurements performed on a pure-argon plasma and on the Ar-Mg plasma. No detectable variation of the continuum level is found, showing that the plasma parameter values are practically unaffected by the presence of magnesium with such a very weak concentration.

IV. MEASUREMENT OF STARK PROFILES: DATA REDUCTION

All profile measurements are performed end-on on the arc axis. Owing to the small beam aperture and field-stop values, the radial Mg inhomogeneities do not affect the plasma region contributing to the measured axial radiation. The primary profile data stored at the output of the digital voltmeter obviously deviate from a pure Stark profile due to the influence of several competing effects: optical depth effects, instrumental, Doppler, resonance, and van der Waals broadening (see, for example, Konjević and Wiese[36] for a thorough discussion of this point). Great care is taken to reduce the influence of the first effect to a negligible level, while the others are taken into account by an appropriate data analysis and the measurement of the instrumental broadening.

A. Optical depth

A non-negligible optical depth in the investigated line gives rise to an additional broadening, though the Lorentzian shape of the line is only slightly altered.[37] Baur and Cooper[38] and Truong-Bach and Drawin[39] have shown that an optical depth τ in the line peak leads approximatively to

an additional Lorentzian width $l_\tau = \tau l/4$ (τ remaining $\lesssim 1$, the source function being constant along the line of sight), where l is the true Lorentzian width of the line.

With the ratio of the peak intensities of the Mg II resonance doublet depending strongly on the optical depth, it is used to select the range of magnesium concentration for which both lines remain thin. The furnace temperature is thus fixed so that the ratio reaches nearly the value 2:1 corresponding to the optically thin case as expected from L-S coupling calculations.[40] Then direct measurements of the optical depth at the peaks of the investigated lines are performed through a double-path method by focusing the radiation emitted from the anode side onto the arc axis with the concave mirror M_2. For τ values lower than 0.05 it is difficult to extract the line from the continuum and the stability of the Mg resonance lines becomes problematic. The data-acquisition process is started when the measured optical depth value is between 0.05 and 0.1. The systematic overestimation of the Lorentzian width due to self-absorption effects is then lower than 2.5%.

B. Deconvolution procedure

The various competing broadening mechanisms act through Gauss or Lorentz shapes. A Voigt profile analysis of the experimental data is therefore justified. All the measured intensity points within a free spectral range of the FPI are fitted by a least-squares analysis accounting for the overlapping of the two adjacent interference orders. The fitting function

$$V(\lambda)+V(\lambda-\Delta\lambda_{\mathrm{FSR}})+V(\lambda+\Delta\lambda_{\mathrm{FSR}})+C$$

is the sum of three approximate Voigt functions[17] and of a constant continuum. The Whiting's analytical approximation[17] gives the Voigt profile as a function of four independent parameters, the Voigt and Lorentz full widths, the position and intensity of the line peak which are then the free parameters of the least-squares fit, together with the continuum value C. The uncertainties of the least-squares parameters, essentially due to the noise in the intensity data, are the standard deviations computed by the fitting code.[41] For the Voigt and Lorentz widths they are typically of the order of 2% and 15%, respectively. A typical fitted profile is given for illustration in Fig. 3 in a reduced-wavelength scale.

The intrinsic Lorentzian width of the line is simply obtained by subtracting the Lorentzian width of the instrumental profile from the measured Lorentzian width given by the least-squares analysis. Stark (electrons and ions), resonance, and van der Waals broadening contribute to this intrinsic Lorentzian width. A theoretical estimate[28] shows that the resonance contribution is completely negligible. The van der Waals broadening estimated following Ref. 28 amounts to 4% at most and is subtracted from the intrinsic width. Then the final value is the total (electrons + ions) Stark width. It is to be noted that, for the lines studied here, the ions contribute to the Stark broadening in the impact regime,[4,5,7] i.e., the ionic contribution, as well as the electronic contribution is proportional to the electron density.

The full Gaussian width g may be calculated from the Voigt and Lorentz full widths v and l through the relation $g=[v(v-l)]^{1/2}$.[17] Due to the difference term, the uncertainty on g is quite important and a temperature determination based on the Doppler width is too imprecise ($\Delta T/T$ between 20 and 50%) to be used as a valuable diagnostic method or check.

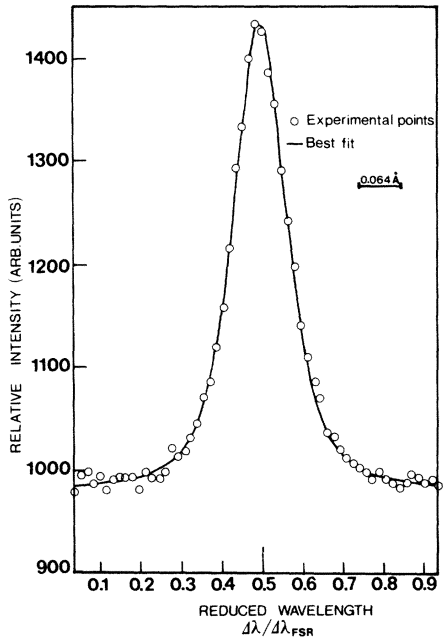

FIG. 3. Typical measured profile of the Mg II 2802.70-Å line at 100 A ($n_e = 1.28\times10^{17}$ cm^{-3}). The plate separation is 0.61 mm ($\Delta\lambda_{\mathrm{FSR}} = 0.6439$ Å). The standard deviations on the Voigt and Lorentz widths given by the fitting code are 1.38% and 9.89%, respectively.

TABLE IV. Measured Stark widths of Mg I and Mg II resonance lines.

Arc current (A)	80			100			140		
Temperature (K)	12970			13370			14260		
Electron density (10^{17} cm^{-3})	1.10			1.28			1.64		
Neutral density (10^{17} cm^{-3})	3.51			2.97			1.89		
	Mg I 2852 Å	Mg II 2795 Å	Mg II 2802 Å	Mg I 2852 Å	Mg II 2795 Å	Mg II 2802 Å	Mg II 2795 Å		Mg II 2802 Å
van der Waals full width (Å)	0.00225	0.00149	0.00149	0.00195	0.00129	0.00129	0.00084		0.00084
Stark full width (Å)	0.054	0.048	0.043	0.071	0.057	0.053	0.077		0.065
Random error (%)	±2.5	±7.0	±12.0	±3.5	±3.5	±4.5	±3.5		±5.0
Systematic error (%)	+1,−5	+1,−5	+1,−5	+1,−5	+1,−5	+1,−5	+1,−5		+1,−5
Stark full width (Å) normalized to $n_e=10^{17}$ cm^{-3}	0.049	0.044	0.039	0.055	0.045	0.041	0.047		0.039
Random error (%)	±3.5	±7.5	±12.5	±4.0	±4.0	±5.0	±4.0		±5.5
Systematic error (%)	+21,−25	+21,−25	+21,−25	+21,−25	+21,−25	+21,−25	+21,−25		+21,−25

V. RESULTS AND DISCUSSION

The experimental widths of the investigated lines are listed in Table IV. For each line and for a given arc current, ten profiles have been independently measured.

A. Error analysis

Random uncertainties. The most important source of random error comes from the noise in the experimental profiles. We quote the magnitude of the corresponding uncertainty in the Lorentzian width l_{meas} (in the reduced-wavelength scale) as the standard deviation associated with it by the least-squares fitting procedure.[41] In addition, a $\pm 2\%$ random error in the determination of N (the free spectral range in arbitrary units) and a $\pm 1\%$ random error in the measure of the FPI plate separation are taken into account. Random uncertainties associated with the instrumental width l_I ($\Delta l_I / l_I = \pm 1.5\%$) are completely negligible as l_{meas}/l_I is always larger than 7. Random errors are added in quadrature to give the relevant uncertainty $\Delta l/l$ with $l=(l_{\text{meas}}-l_I)\lambda^2/2e$. The distribution of the measured $(l,\Delta l/l)$ yields a weighted mean value $\bar{l}$ and an error bracket[42] given in Table IV (after subtraction of the van der Waals width).

The random uncertainty on the electron-density value is discussed in Sec. III. The final random error on the normalized Stark width (at $n_e=10^{17}$ cm^{-3}) is also given in Table IV.

Systematic uncertainties. The main systematic error occurs in the plasma parameter determination and is discussed in Sec. III. Nonperfect linearity of the spectral scanning of the FPI amounts to $\pm 1\%$ in l_{meas}. Residual optical depth effects ($\tau < 0.1$) lead to an overestimation of l_{meas} of 2.5% at most. The deviations from the true Voigt profile of the analytic approximation used remain small.[17] The error in the Voigt width is less than 1% throughout the range from pure Gaussian to pure Lorentzian profiles and the error in the Lorentz width is expected to be small relative to other sources of error. Systematic uncertainties in l_I ($\Delta l_I/l_I = +1\%, -7\%$) induce an overestimation of l of the order of 1% at most ($l_{\text{meas}}/l_I \geq 7$). Finally the various systematic errors are added linearly and amount to $(+1\%,-5\%)$ for the Stark width and to $(+21\%,-25\%)$ for the normalized Stark width at $n_e=10^{17}$ cm^{-3}.

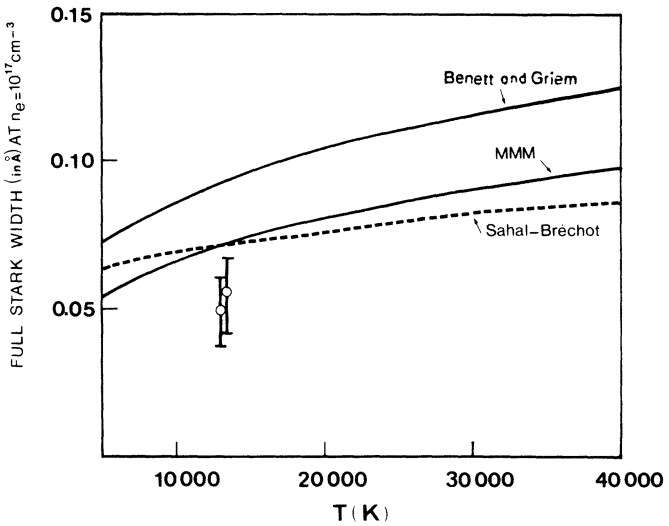

FIG. 4. Comparison of Mg I results with published data. The experimental error bars represent the systematic error.

B. Mg I results ($3s^2\,{}^1S$-$3s\,3p\,{}^1P^o$ at 2852.13 Å)

The semiclassical impact calculations of Benett and Griem,[3] Sahal-Bréchot,[4] and the model microfield method (MMM) semiclassical results of Brissaud *et al.*[5] are displayed in Fig. 4 with our experimental points. To our knowledge no other experimental results are available for this line. All the theoretical results include the ionic broadening which generally accounts for no more than 10% of the total width.[3,5] Sahal-Bréchot, who takes into account the elastic quadrupolar contribution in the ionic impact broadening, finds an ionic width reaching 30% of the total width.

The experimental points lie 20% lower than Sahal-Bréchot and MMM calculations, which coincide fortuitously near 13 000 K. The disagreement with Benett and Griem results reaches 40% of the calculated width. Dominant angular momenta of the colliding electron are of the order of unity in this case.[43] Therefore short-range effects are important and the breakdown of semiclassical treatments is a possible explanation of the theory-experiment disagreement revealed here.

C. Mg II results ($3s\,{}^2S_{1/2}$-$3p\,{}^2P^o_{1/2,3/2}$ at 2802.70 and 2795.53 Å)

Our experimental results are displayed in Fig. 5 together with existing calculations[6,8–11] and previous experimental determinations.[7–9,12,13] As in the case of the Mg I resonance line our values lie, respectively, 40 and and 50% lower than the semiclassical calculations of Sahal-Bréchot[9] (including correction for resonances of cross sections and ionic broadening) and of Jones, Benett, and Griem[6] (electronic broadening only).

The previous experimental studies, beside those of Chapelle and Sahal-Bréchot[7] and Fleurier *et al.*,[9] were all performed with pulsed sources. Except for Jones *et al.*,[12] they all made use of conventional grating monochromators. The corresponding results lie about a factor of 2 higher than the present results and fit particularly well the Jones, Benett, and Griem calculations, with the exception of Roberts and Barnard,[8] whose results are in complete agreement with ours. At this point it is to be noted that our primary-width data, i.e., the width of the Voigt profile before any deconvolution procedure, are also a factor of 2 greater than the final Stark-width values. This suggests that a too rough determination of the instrumental profile of the grating monochromators and/or an inaccurate deconvolution procedure may explain, at least partly, the divergencies between the experiments. Possible optical depth effects cannot be excluded either, the optical depth being generally not measured but only indirectly checked.

A difference between the widths of the two lines of the Mg II resonance doublet is systematically observed in our measurements, though it remains within the respective error bars. Such a width variation within the lines of a multiplet is expected from quantum-mechanical calculations,[10] but the calculated effect (the $J=\frac{1}{2}\rightarrow\frac{1}{2}$ line wider than the $J=\frac{1}{2}\rightarrow\frac{3}{2}$ line) is opposite the observed one. Optical depth effects are stronger in the more intense

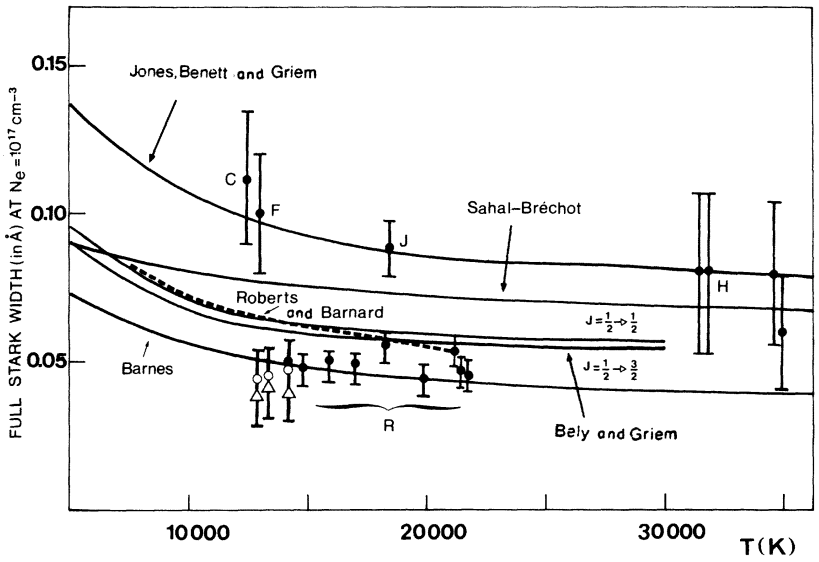

FIG. 5. Comparison of Mg II results with published data. C, Chapelle and Sahal-Bréchot (Ref. 7); F, Fleurier *et al.* (Ref. 9); J, Jones *et al.* (Ref. 12); H, Hadžiomerspahić *et al.* (Ref. 13); R, Roberts and Barnard (Ref. 8). ○ and △ : this experiment for the $J=\frac{1}{2}\rightarrow\frac{3}{2}$ line and the $J=\frac{1}{2}\rightarrow\frac{1}{2}$ line, respectively (the error bars represent the systematic error).

$J=\frac{1}{2}\rightarrow\frac{3}{2}$ line than in the $J=\frac{1}{2}\rightarrow\frac{1}{2}$ but the possible 2.5% overestimation of the width (see Sec. IV A) is not sufficient to explain the total systematic difference.

The quantum-mechanical calculations are still afflicted with inaccuracies connected with extrapolation procedures of elastic scattering matrix elements across inelastic thresholds and with the account of very few perturbing levels. Nevertheless the present results seem to indicate that such quantum calculations give more realistic results than the semiclassical ones for the Mg II resonance doublet. Quantum results for the Mg I resonance line would be of interest in view of the present study.

We thank sincerely Sylvie Sahal-Bréchot for providing us with unpublished results.

[1]Proceedings of the 4th Colloquium on Astrophysics: High Resolution Spectrometry, edited by M. Hack, Trieste, Italy, July, 1978 (unpublished).
[2]Proceedings of the Second IUE Conference, compiled by B. Battrick and J. Mort, Tübingen, Germany, March, 1980, ESA SP-157 (unpublished).
[3]S. M. Benett and H. R. Griem, University of Maryland Technical Report No. 71-097 (unpublished).
[4]S. Sahal-Bréchot, Astron. Astrophys. 1, 91 (1969); 2, 322 (1969); and private communication.
[5]A. Brissaud, C. Goldbach, J. Léorat, A. Mazure, and G. Nollez, J. Phys. B 9, 1147 (1976).
[6]W. W. Jones, S. M. Benett, and H. R. Griem, University of Maryland Technical Report No. 71-128 (unpublished).
[7]J. Chapelle and S. Sahal-Bréchot, Astron. Astrophys. 6, 415 (1970).
[8]D. E. Roberts and A. J. Barnard, J. Quant. Spectrosc. Radiat. Transfer 12, 1205 (1972).
[9]C. Fleurier, S. Sahal-Bréchot, and J. Chapelle, J. Quant. Spectrosc. Radiat. Transfer 17, 595 (1977).
[10]O. Bely and H. R. Griem, Phys. Rev. A 1, 97 (1970).
[11]K. S. Barnes, J. Phys. B 4, 1377 (1971).
[12]W. W. Jones, A. Sanchez, J. R. Greig, and H. R. Griem, Phys. Rev. A 5, 2318 (1972).
[13]D. Hadžiomerspahić, M. Platiša, N. Konjević, and M. Popović, Z. Phys. 262, 169 (1973).
[14]Smithsonian Physical Tables, prepared by W. E. Forsythe (Smithsonian Institution, Washington, D. C. 1954), p. 364.
[15]R. Chabbal, Rev. Opt. 37, 501 (1958).
[16]R. A. Day, Appl. Opt. 9, 1213 (1970).
[17]E. E. Whiting, J. Quant. Spectrosc. Radiat. Transfer 8, 1379 (1968).
[18]H. Magdeburg and U. Schley, Z. Angew. Phys. 20, 465 (1966).
[19]W. L. Wiese, in *Plasma Diagnostic Techniques,* edited by R. H. Huddlestone and S. L. Leonard (Academic,

New York, 1965), p. 311.
[20]J. Hackman, H. Michael, and J. Uhlenbusch, Z. Phys. 250, 207 (1972).
[21]H. Nubbemeyer, J. Quant. Spectrosc. Radiat. Transfer 16, 395 (1976).
[22]R. C. Preston, J. Phys. B 10, 1377 (1977).
[23]P. Baessler and M. Kock, J. Phys. B 13, 1351 (1980).
[24]W. L. Wiese, M. W. Smith, and B. M. Miles, *Atomic Transition Probabilities,* NSRDS-NBS (National Bureau of Standards, Washington, D. C., 1968).
[25]H. Nubbemeyer and B. Wende, Proceedings of the 13th International Conference on Phenomena in Ionized Gases, Berlin, 1977, p. 147 (unpublished).
[26]C. Fleurier and J. Chapelle, Comput. Phys. Commun. 7, 200 (1974).
[27]H. Nubbemeyer, thesis, Freie Universität, Berlin, 1974 (unpublished).
[28]H. R. Griem, *Plasma Spectroscopy* (McGraw-Hill, New York, 1964).
[29]H. W. Drawin, Z. Phys. 228, 99 (1969).
[30]J. B. Shumaker and C. H. Popenoe, J. Res. Natl. Bur. Stand. 76A, 71 (1972).
[31]R. C. Preston, J. Quant. Spectrosc. Radiat. Transfer 18, 337 (1977).
[32]D. Hofsaess, J. Quant. Spectrosc. Radiat. Transfer 19, 339 (1978).
[33]R. Schnapauff, Z. Astrophys. 68, 431 (1968).
[34]E. Schulz-Gulde, Z. Phys. 230, 449 (1970).
[35]C. Goldbach, G. Nollez, and P. Plomdeur, J. Phys. B 10, 1181 (1977).
[36]N. Konjević and W. L. Wiese, J. Phys. Chem. Ref. Data 5, 259 (1976).
[37]N. Konjević and J. R. Roberts, J. Phys. Chem. Ref. Data 5, 209 (1976).
[38]J. F. Baur and J. Cooper, J. Quant. Spectrosc. Radiat. Transfer 17, 311 (1977).
[39]Truong-Bach and H. W. Drawin, J. Quant. Spectrosc. Radiat. Transfer 22, 389 (1979).
[40]B. W. Shore and D. H. Menzel, *Principles of Atomic Spectra* (Wiley, New York, 1968).
[41]J. R. Wolberg, *Prediction Analysis* (Van Nostrand, Princeton, 1967), p. 54.
[42]S. L. Meyer, *Data Analysis* (Wiley, New York, 1975), p. 43.
[43]M. S. Dimitrijević, N. Feautrier, and S. Sahal-Bréchot, J. Phys. B 14, 2559 (1981).